Modeling the Extreme X-ray Spectrum of IRAS 13224-3809

Chia-Ying Chiang
Wayne State University

Dominic Walton, Andy Fabian, Daniel Wilkins, Luigi Gallo

May 2, 2016, Great Lakes Quasar Symposium

Active Galactic Nuclei (AGN)

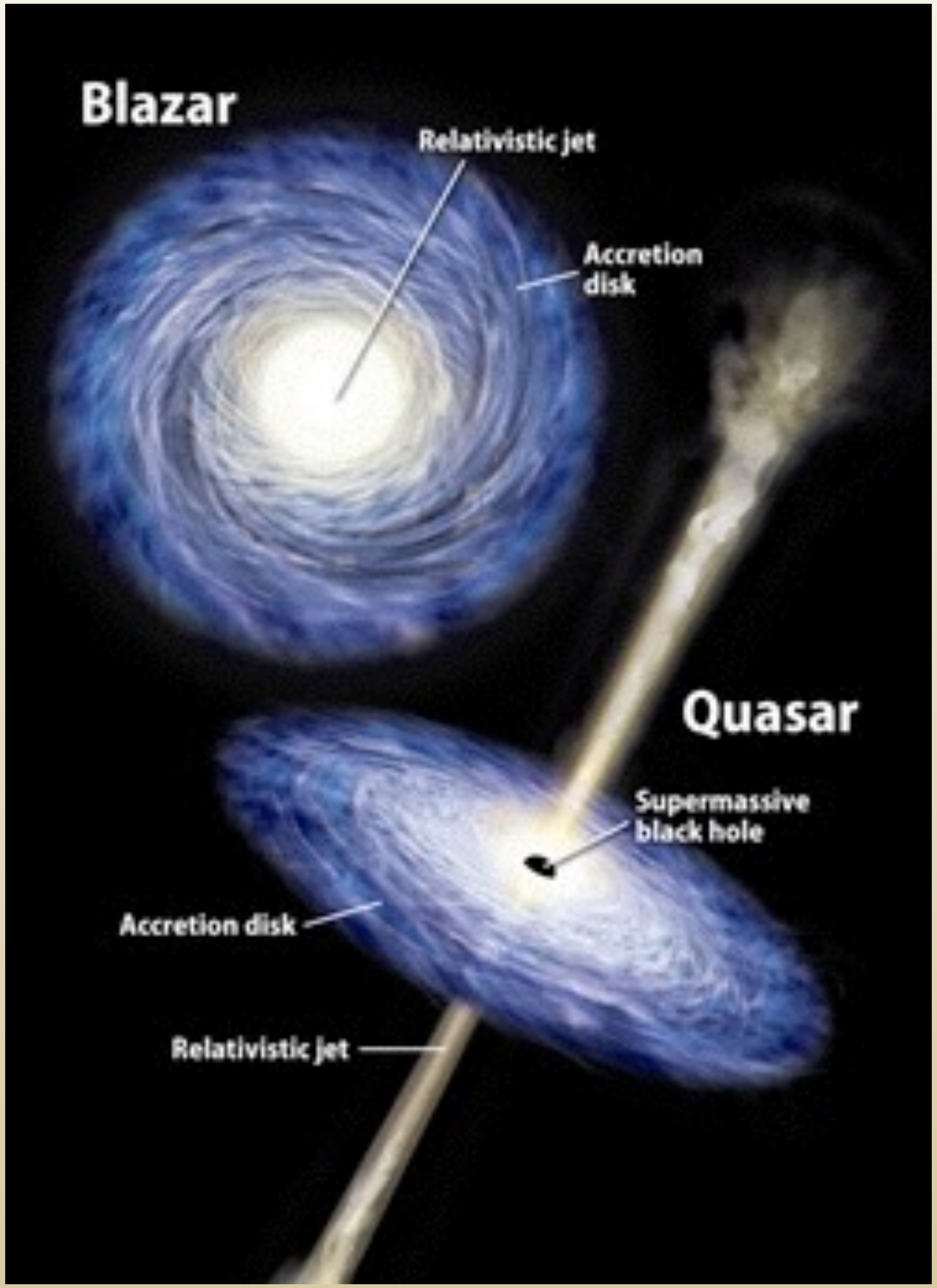

- $L_{AGN} \geq L_{GALAXY}$
- supermassive black holes ($10^5\, M_\odot < M_{BH} < 10^8\, M_\odot$)
- observed in the radio, microwaves, infrared, optical, ultra-violet, X-ray and gamma ray wavebands
- powered via accretion

Geometry

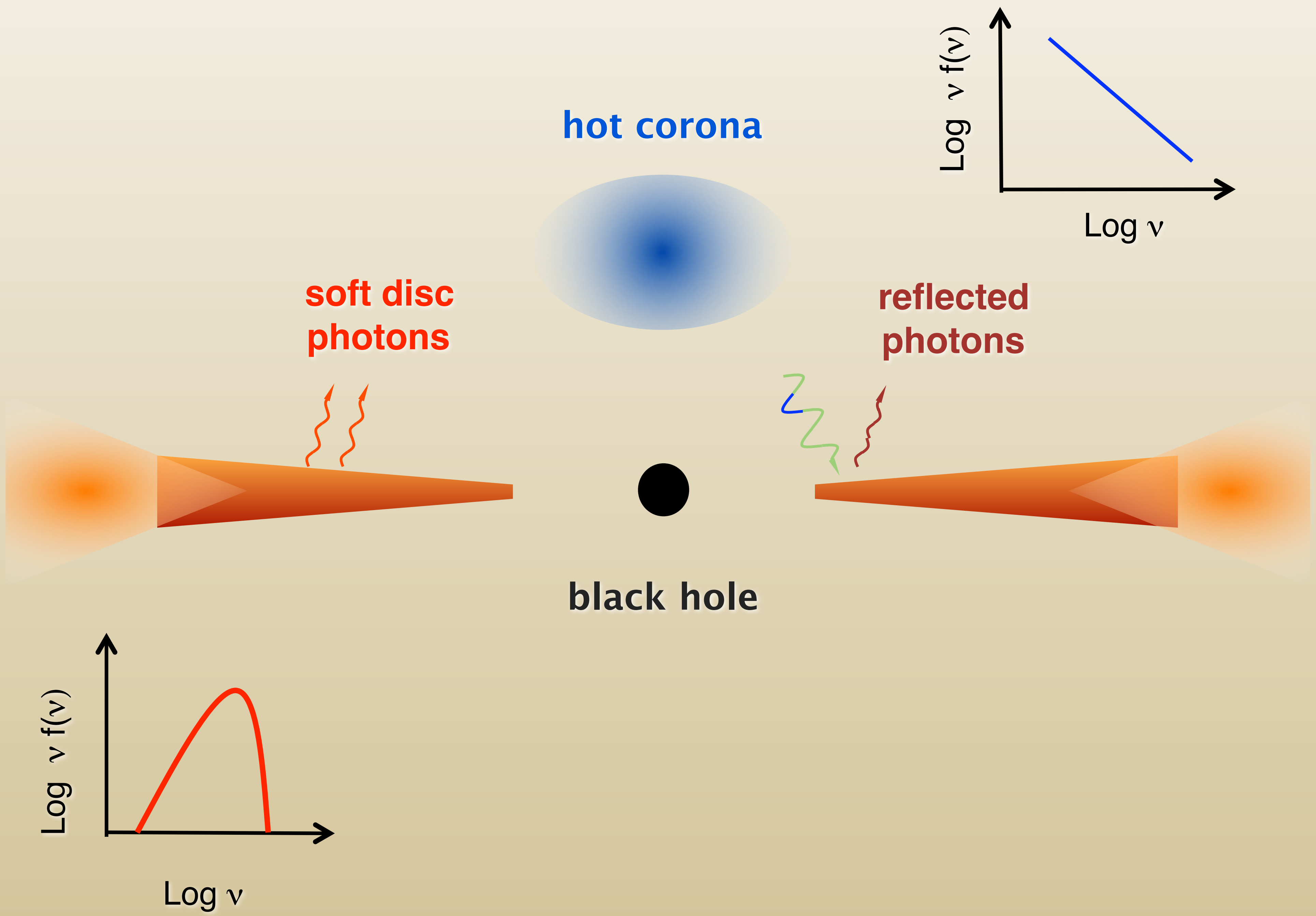

hot corona
Log ν f(ν)
Log ν
soft disc
photons
reflected
photons
black hole
Log ν f(ν)
Log ν

Reflected Spectrum

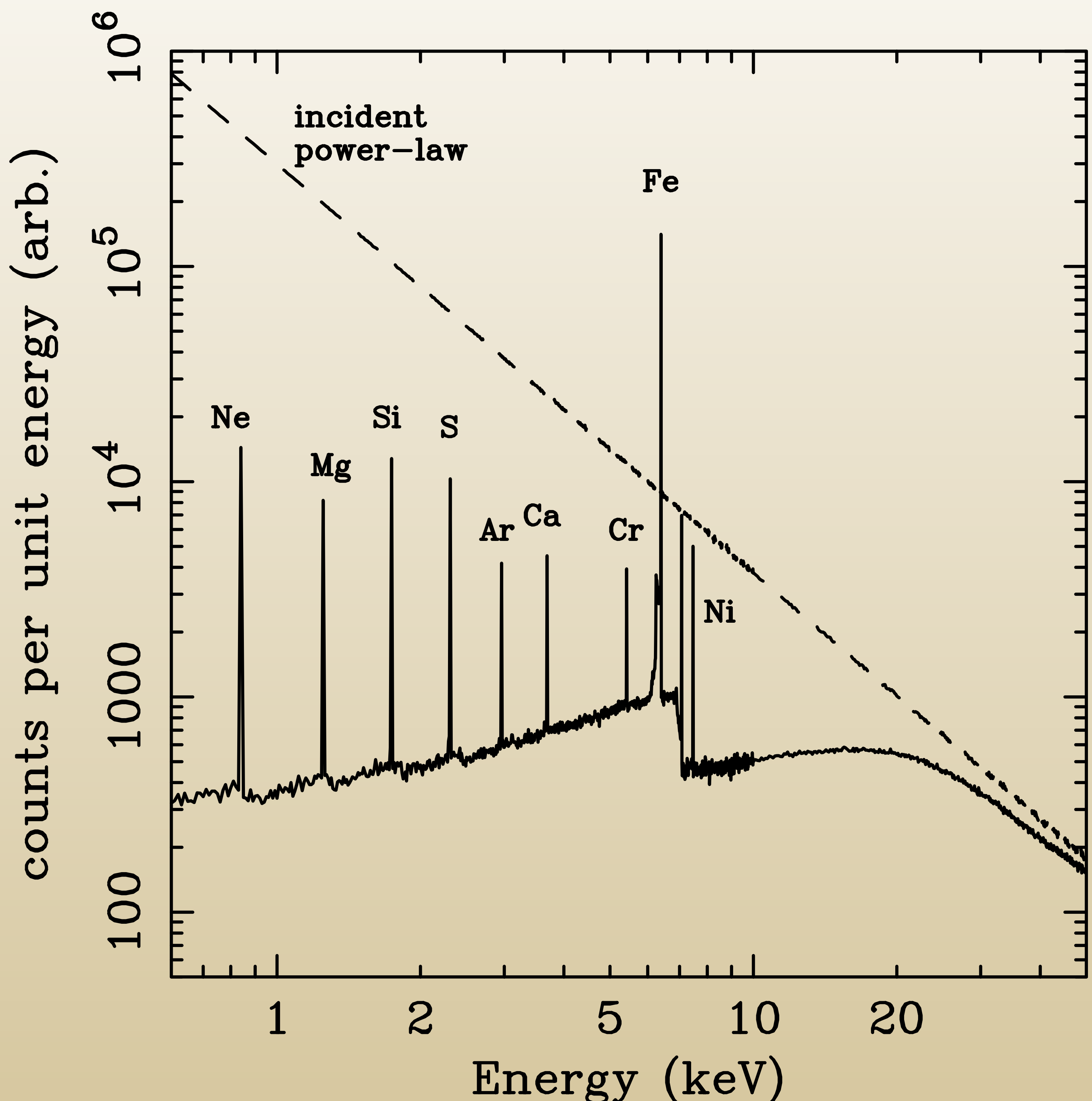

Reynolds (1993)

Relativistic Effects

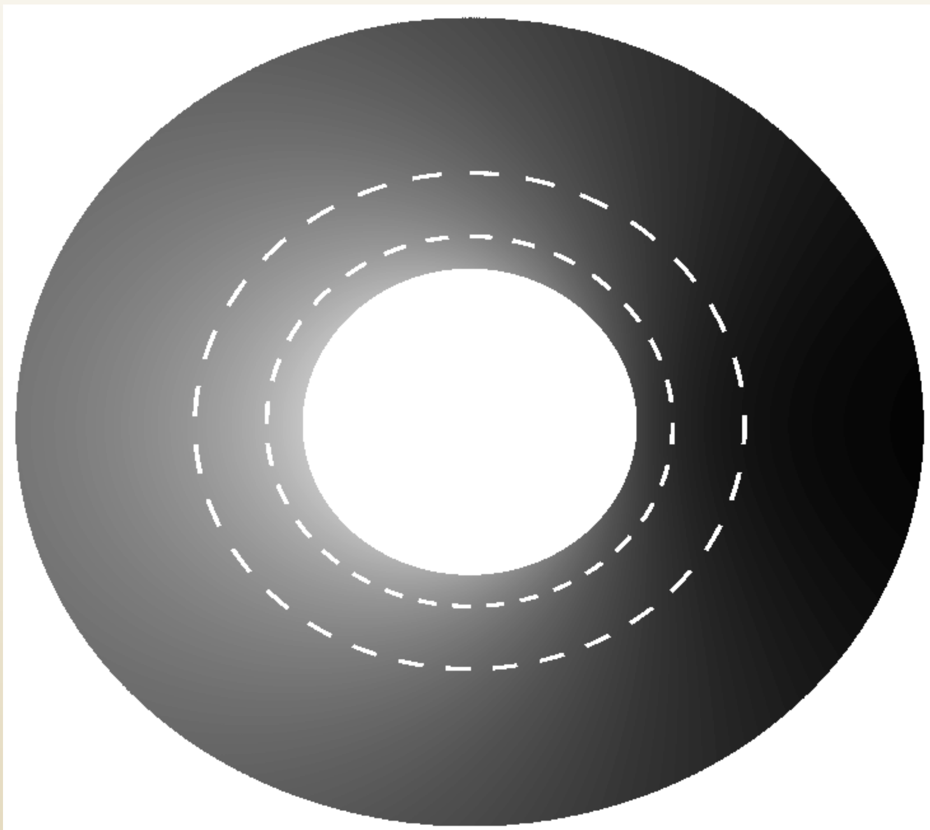

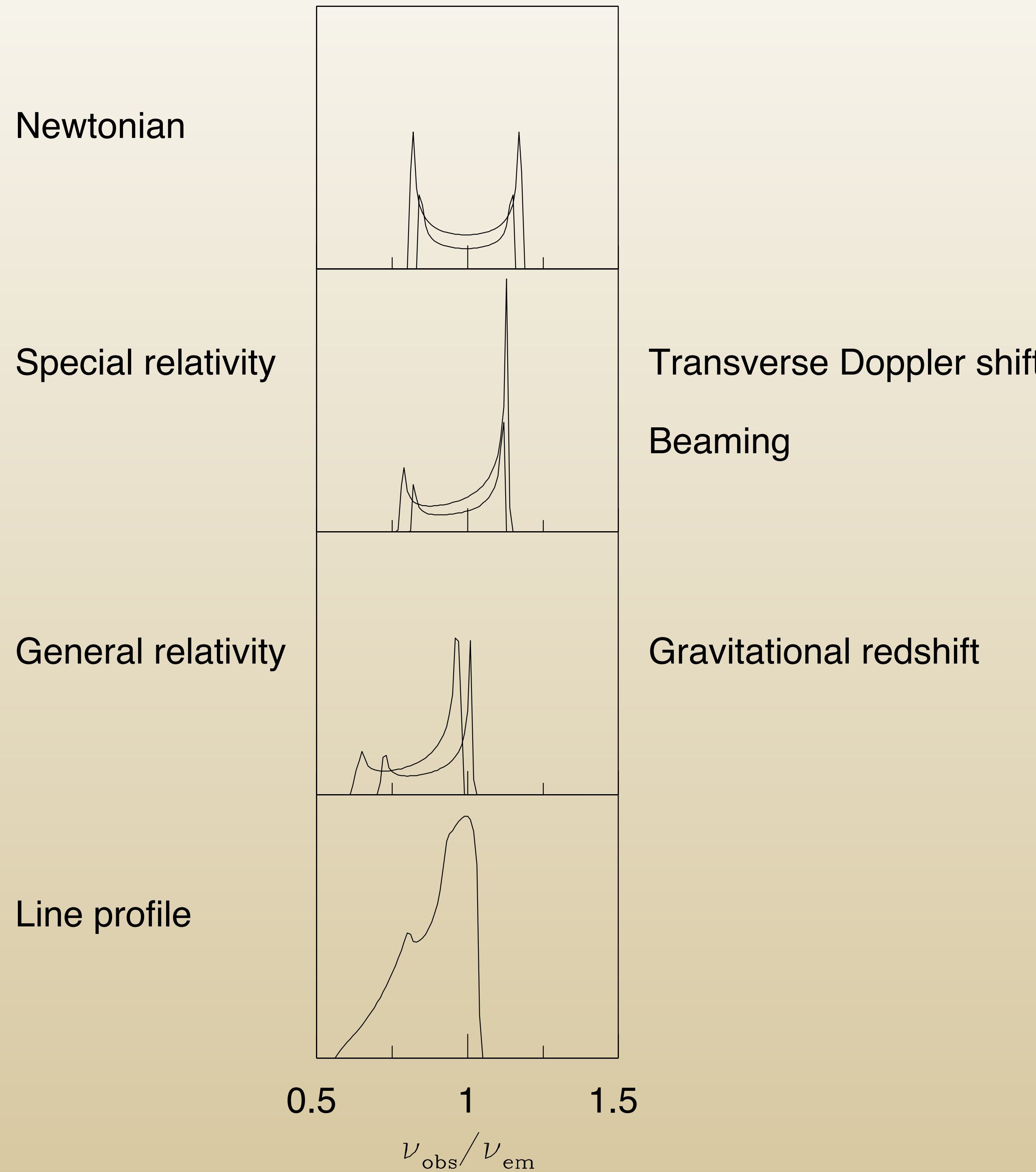

Fabian et al. (2000)

Broad Fe Kα Line

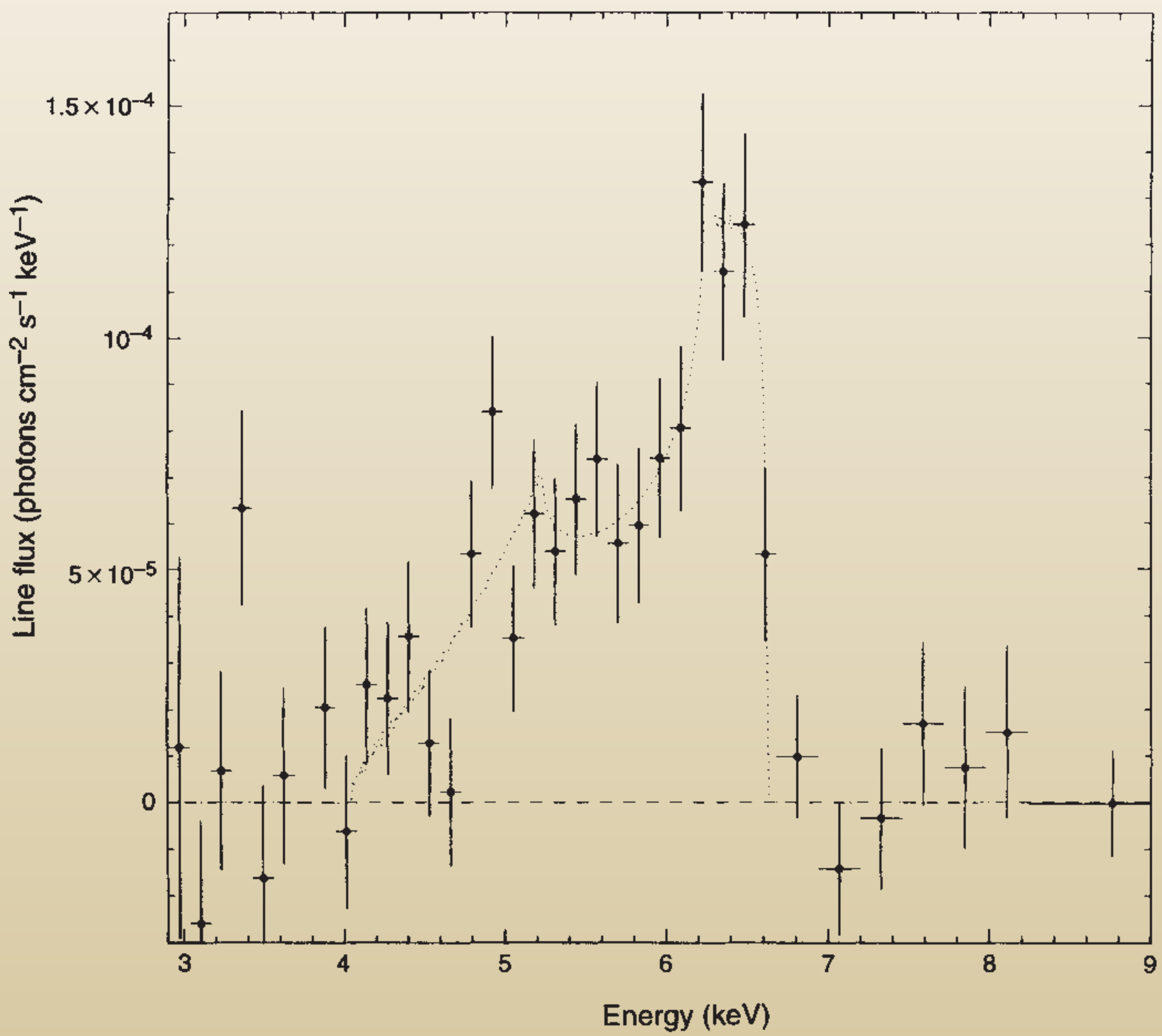

Tanaka et al. (1995)

- Relativistic iron line first discovered in *ASCA* observation of Type I AGN MCG-6-30-15
- Found in both AGN and LXMBs
- Line profile can be used to measure the black hole spin

AGN X-ray Spectrum

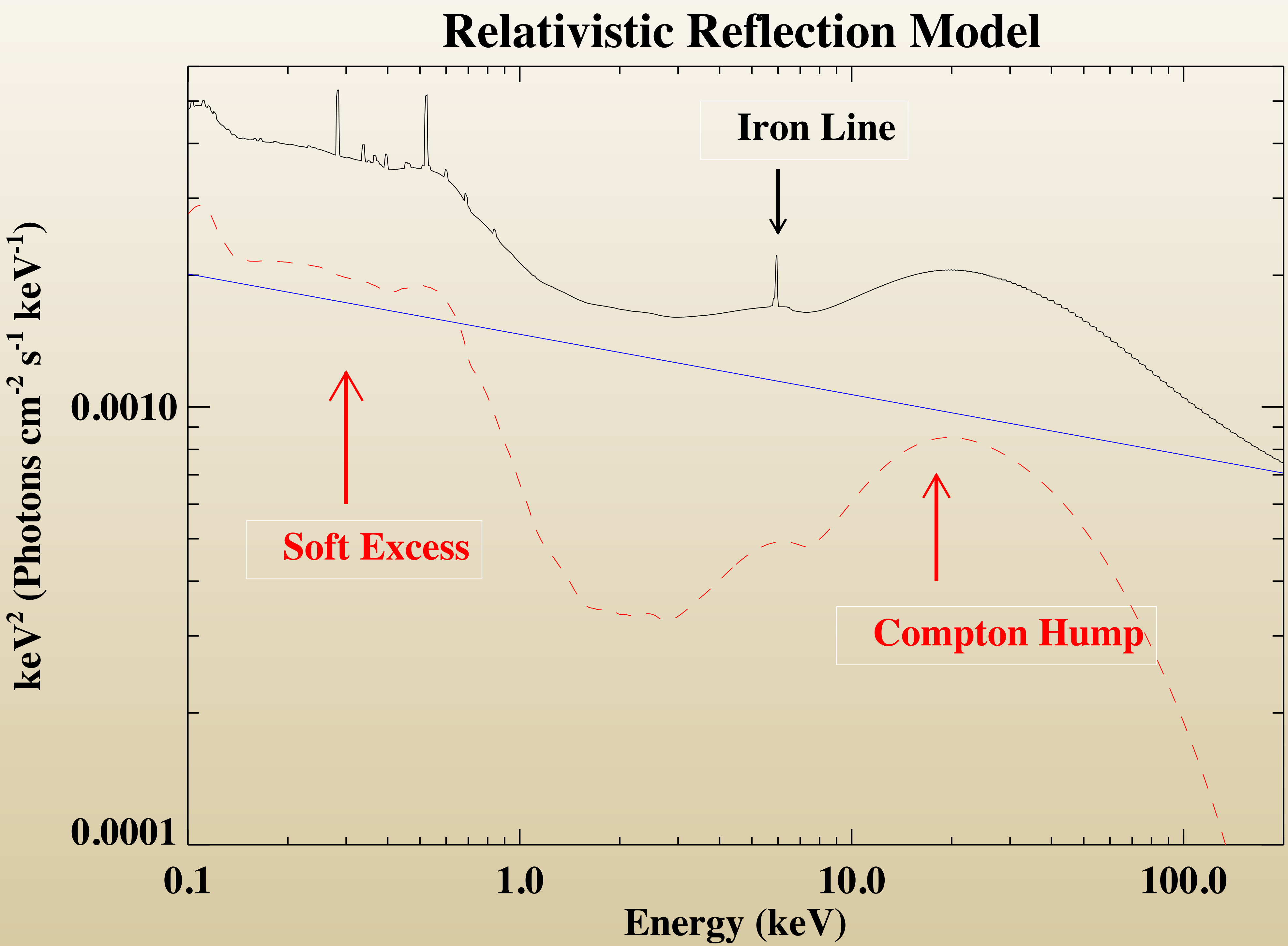

IRAS13224-3809

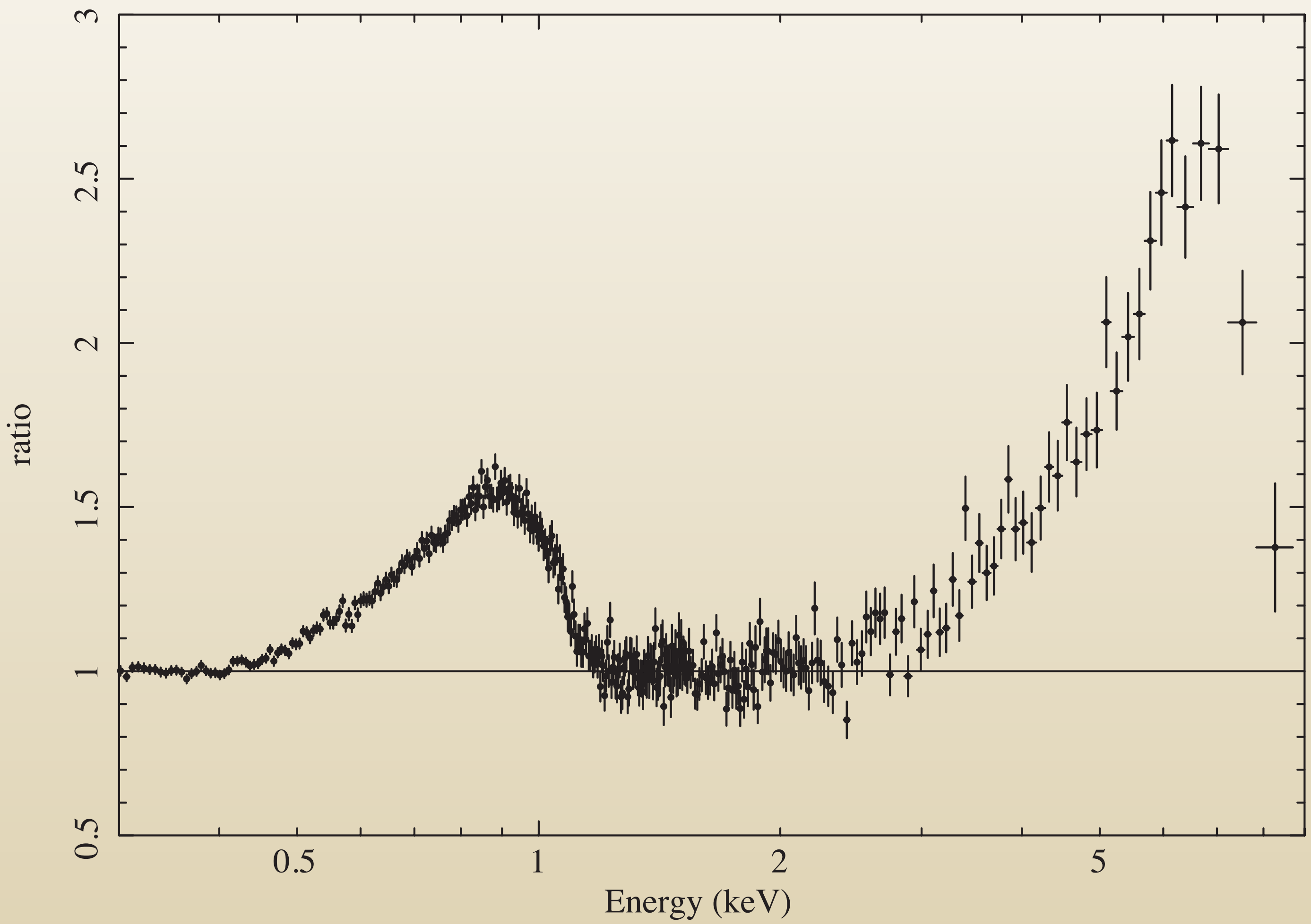

500 ks *XMM-Newton* observation in 2011,
Fabian et al. (2013)

- strong Fe K & Fe L lines,
- sharp edge at ~8 keV
- large variability
- small central black holes, high accreting rates
- high iron abundance

Time-averaged Spectra

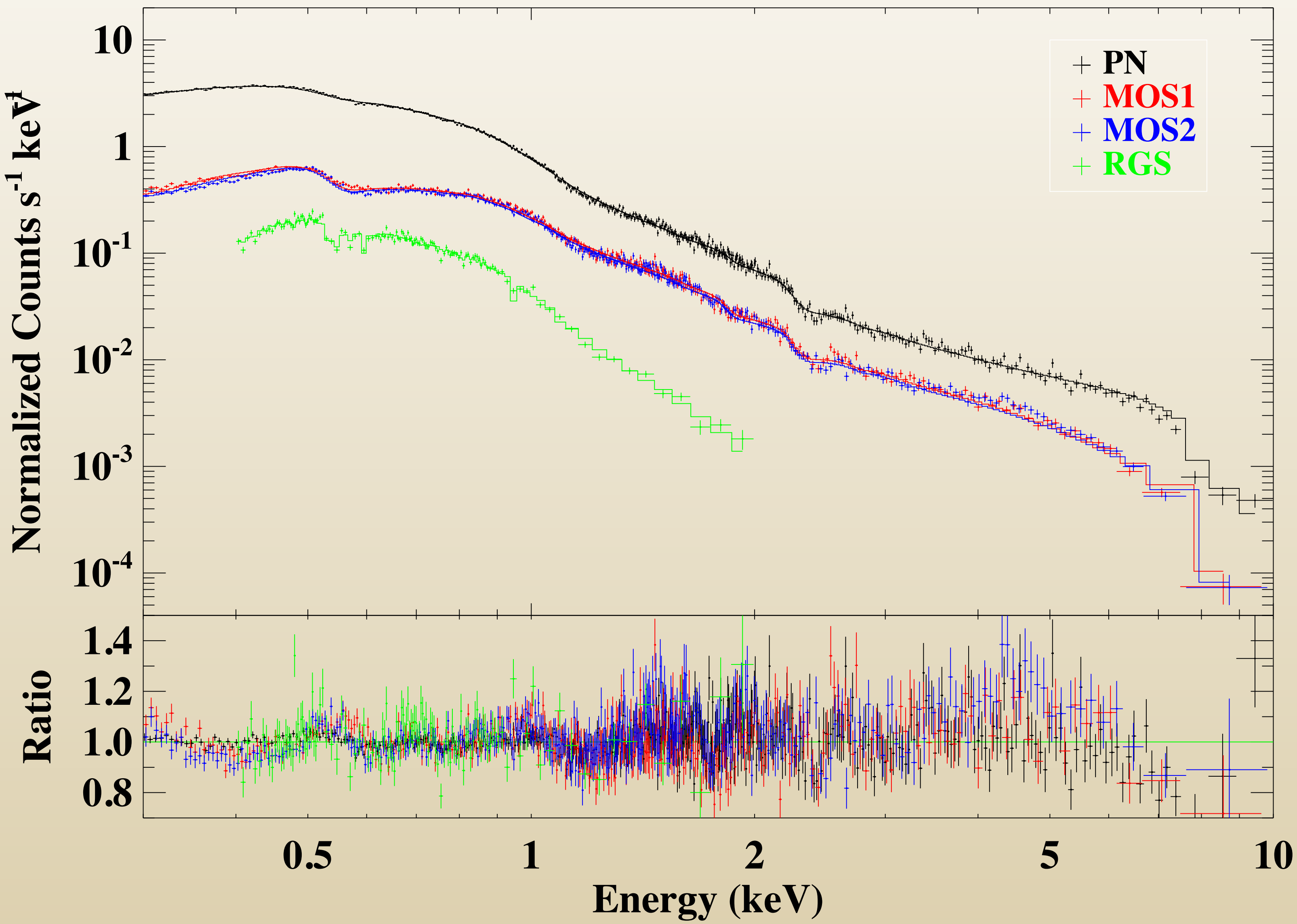

Galactic absorption * (powerlaw + blackbody + blurred reflection)

Chiang et al. (2015)

Time-averaged Spectra

Component	Parameter	Value
TBNEW	Absorption column, $N_{\rm H}$	$6.1^{+0.3}_{-0.1}$
BBODY	Temperature, kT (10^{-2} keV)	$9.3^{+0.1}_{-0.2}$
	Norm	$3.6^{+0.3}_{-0.2} \times 10^{-5}$
	$F_{\rm BB}$	$29.9^{+2.4}_{-1.2}$
POWERLAW	Photon index, Γ	2.71 ± 0.02
	Norm	$(3.8 \pm 0.1) \times 10^{-4}$
	$F_{\rm PLC}$	$43.3^{+1.2}_{-1.1}$
RELCONV	Inner emissivity index, q_1	> 9
	Outer emissivity index, q_2	$3.4^{+0.3}_{-0.2}$
	Spin parameter, a^*	$0.990^{+0.001}_{-0.003}$
	$R_{\rm break}$ ($R_{\rm g}$)	2.1 ± 0.1
	Inclination, i (deg)	$64.6^{+0.6}_{-0.7}$
EXTENDX	Iron abundance /solar, $A_{\rm Fe}$	> 18.1
	Ionization parameter, ξ_1	498^{+4}_{-38}
	Norm_1	$2.2^{+0.1}_{-0.3} \times 10^{-8}$
	Ionization parameter, ξ_2	$20.5^{+0.3}_{-1.1}$
	Norm_2	$5.9^{+0.3}_{-0.9} \times 10^{-6}$
	$F_{\rm RDC}$	$41.0^{+1.3}_{-3.7}$
$\chi^2/d.o.f.$		3633/2892

- rapid-spinning black hole
- high iron abundance
- no absorptions

Chiang et al. (2015)

Time-resolved Spectra

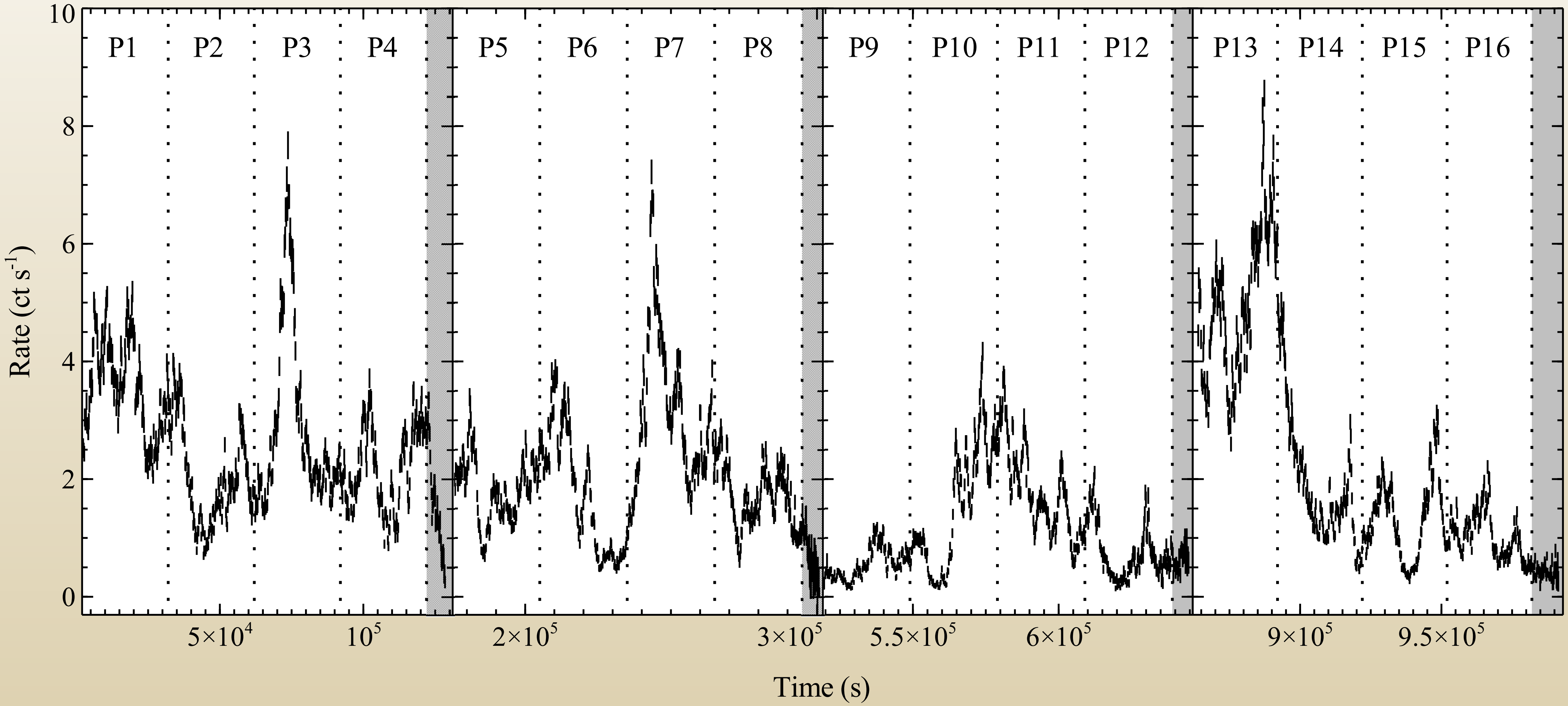

Chiang et al. (2015)

Powerlaw vs. Reflection

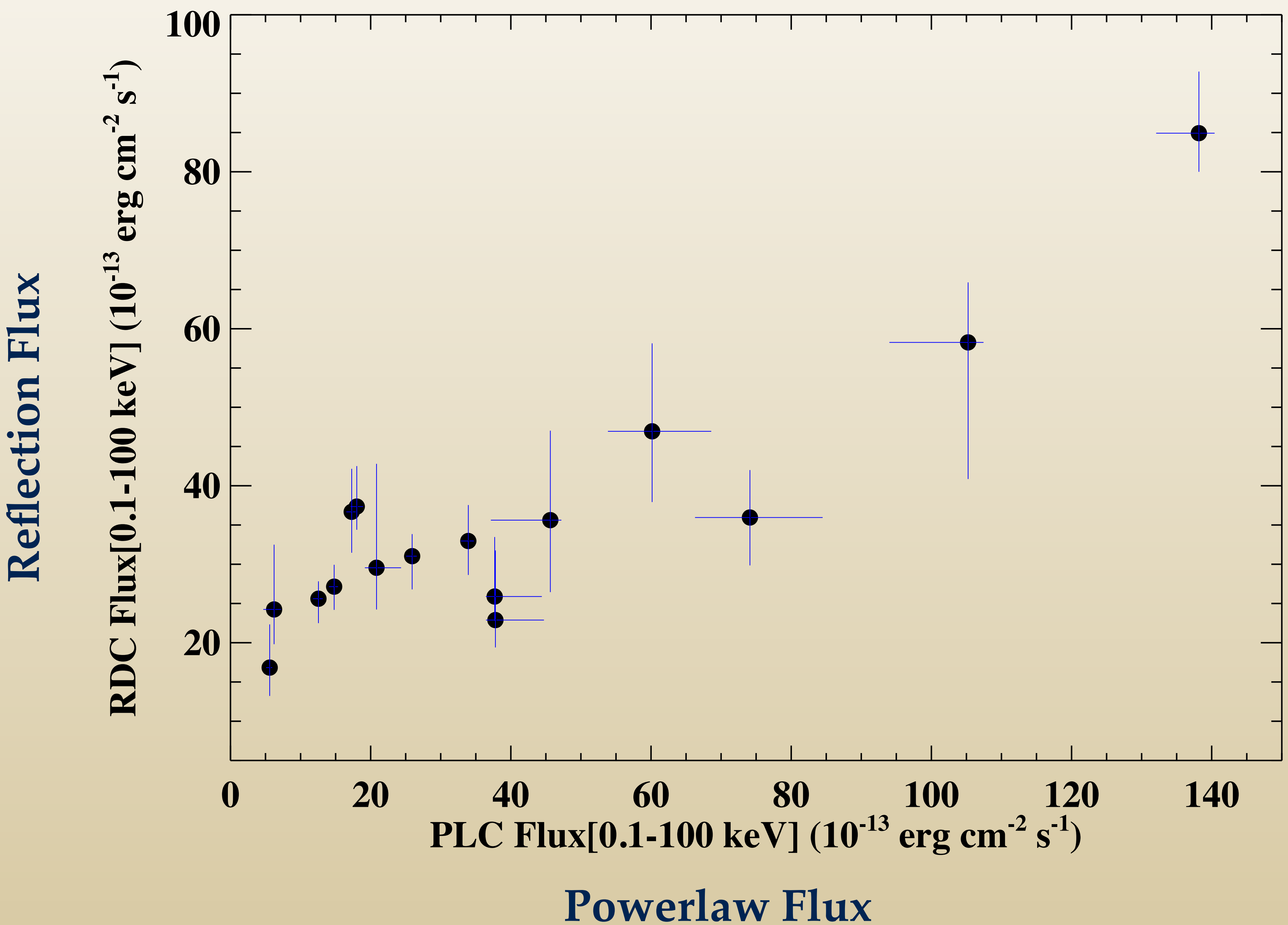

Chiang et al. (2015)

Powerlaw vs. Reflection

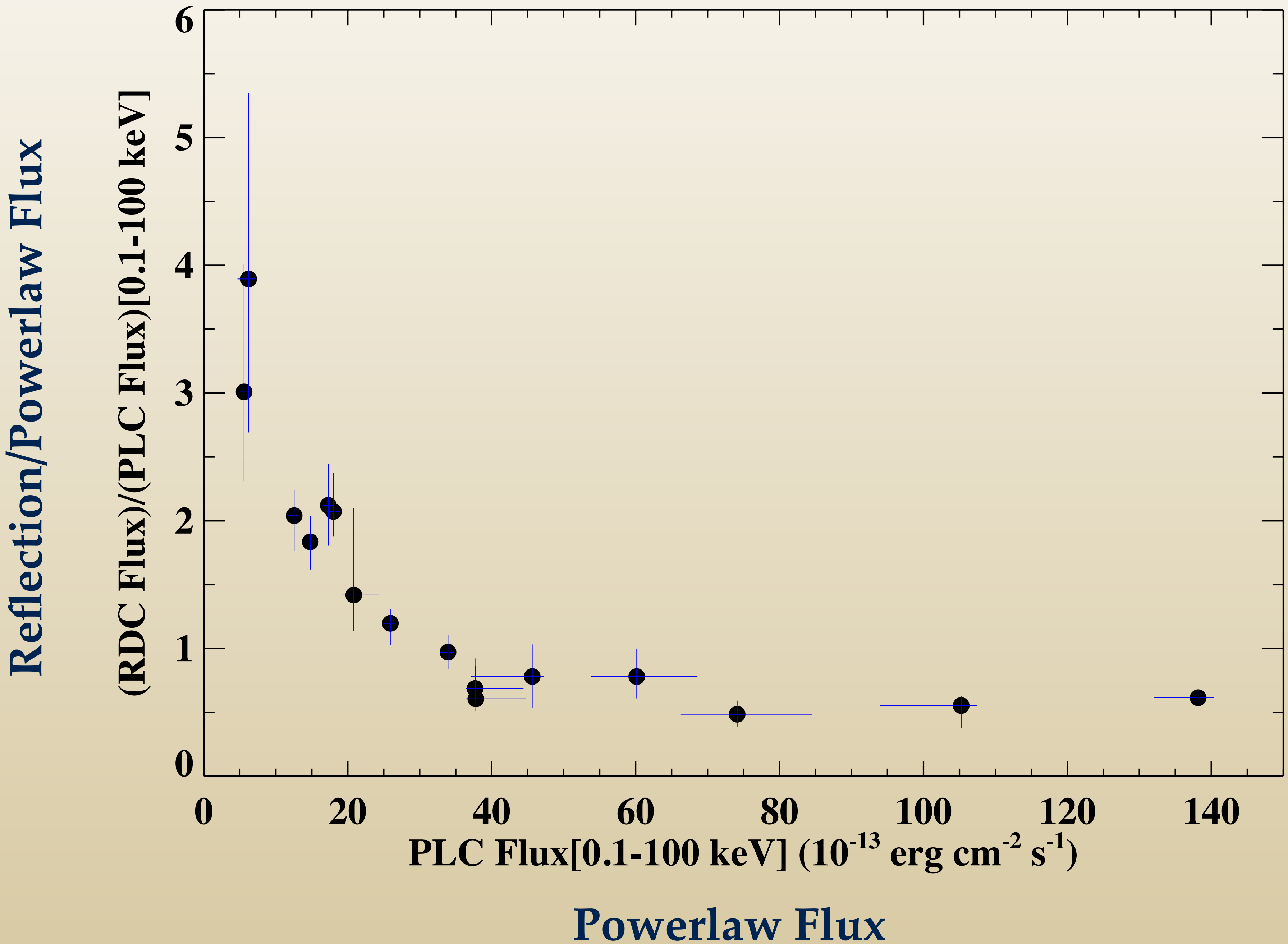

Chiang et al. (2015)

Emissivity Profile

- illumination pattern of accretion disc
- reveals the reflected power per unit area

$$\varepsilon(r) = r^{-q}$$

- $q = 3$ if relativistic effects are not included

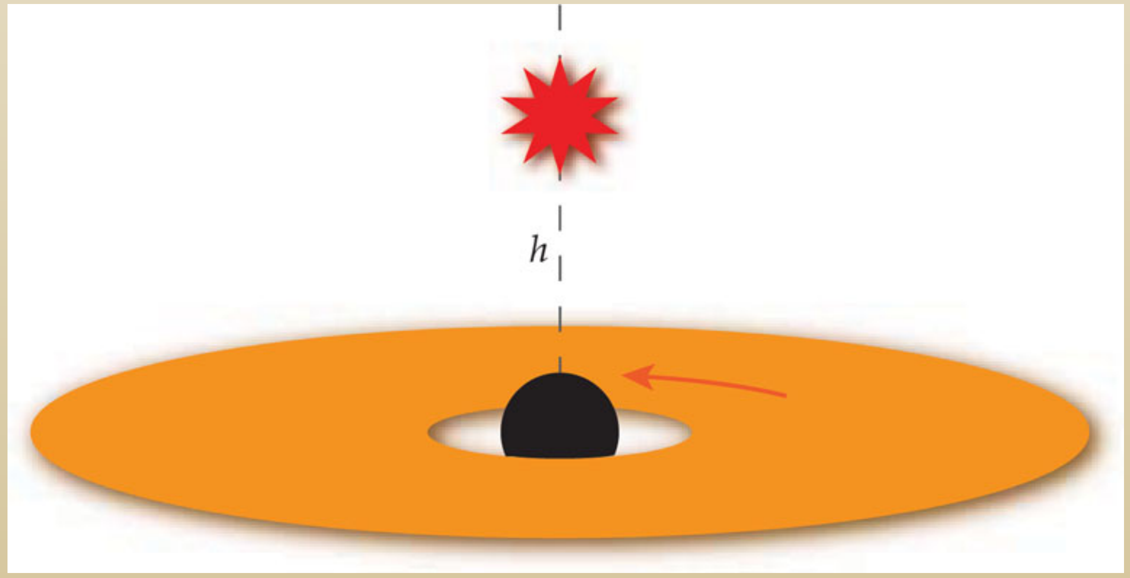

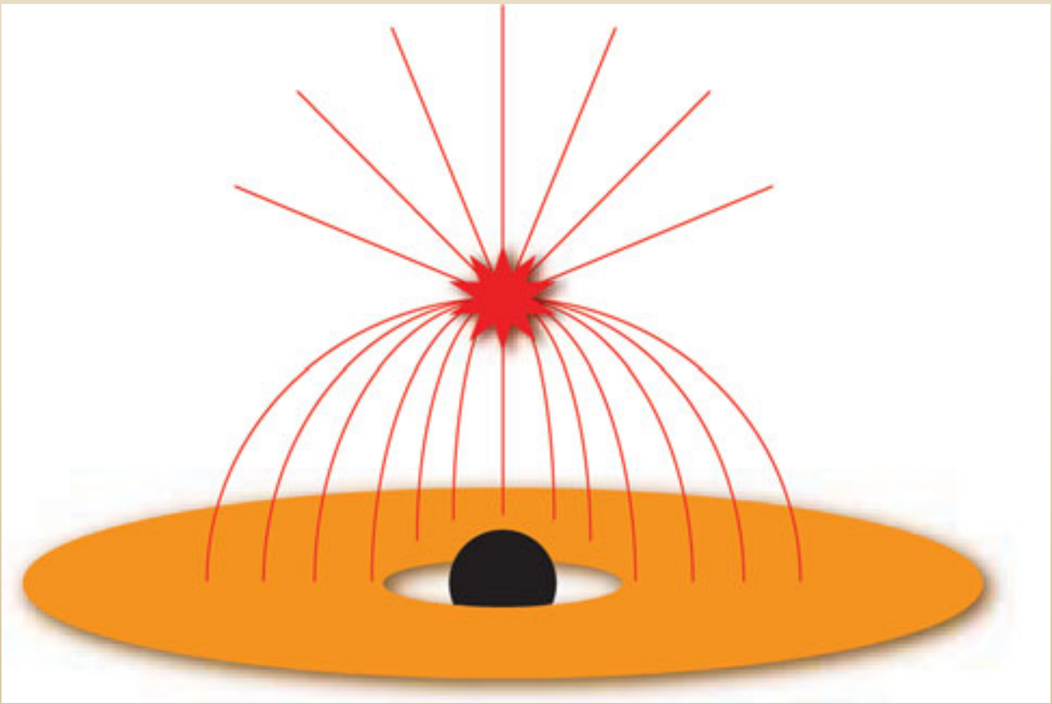

Emissivity Profile

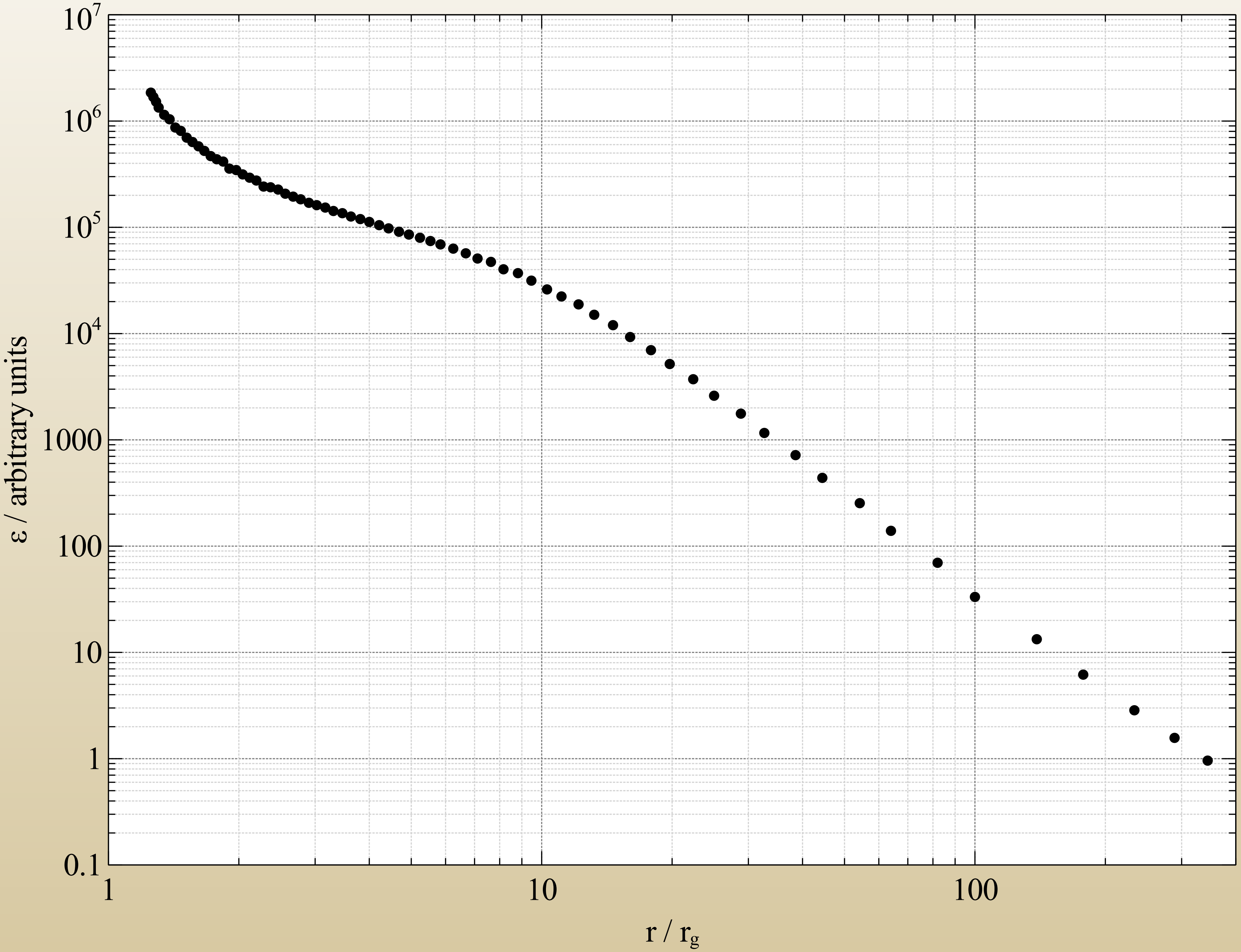

source at $h = 10\ R_G$, Wilkins & Fabian (2012)

Emissivity Evolution

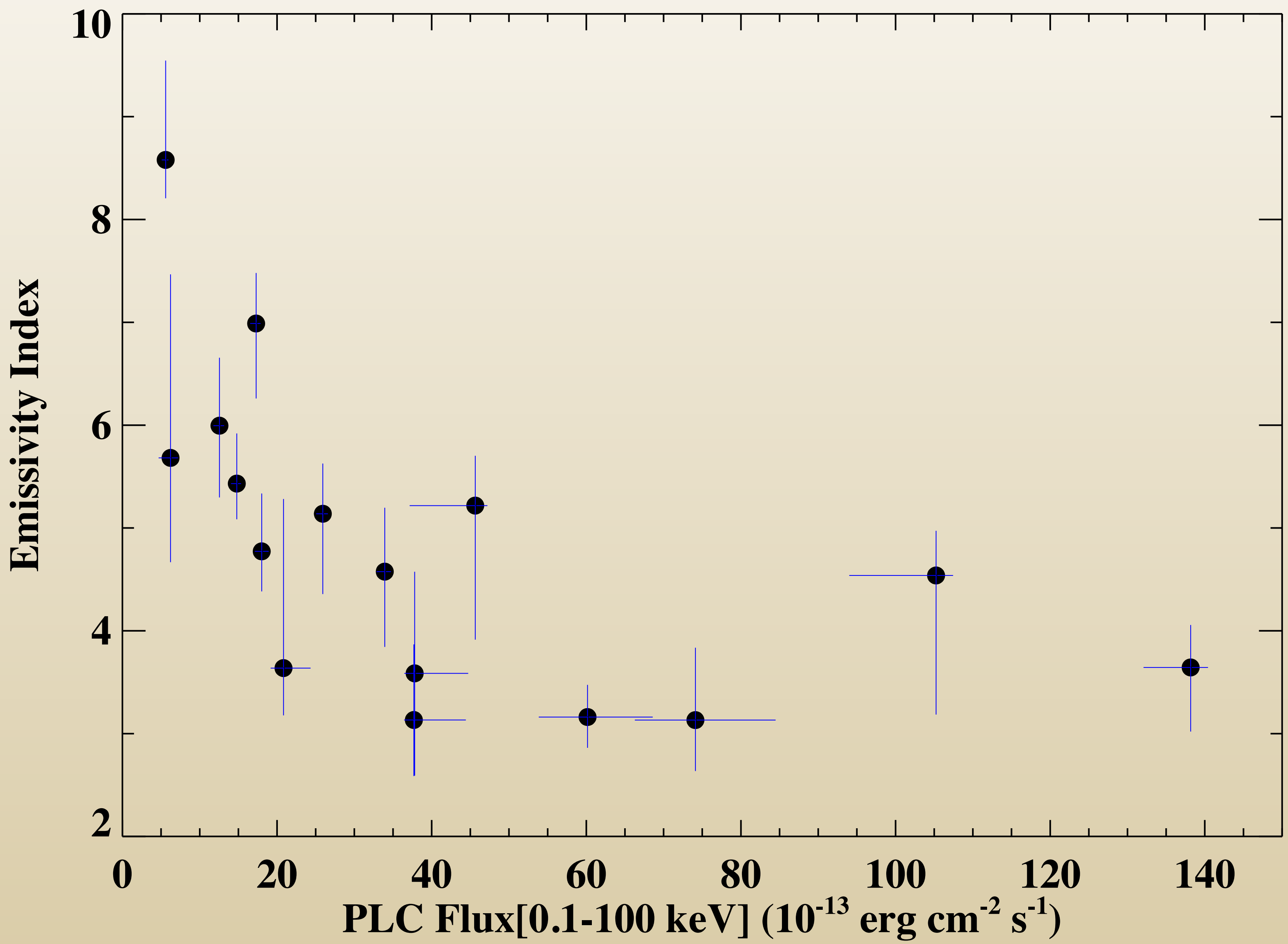

Powerlaw Flux

Chiang et al. (2015)

Lags from different bands

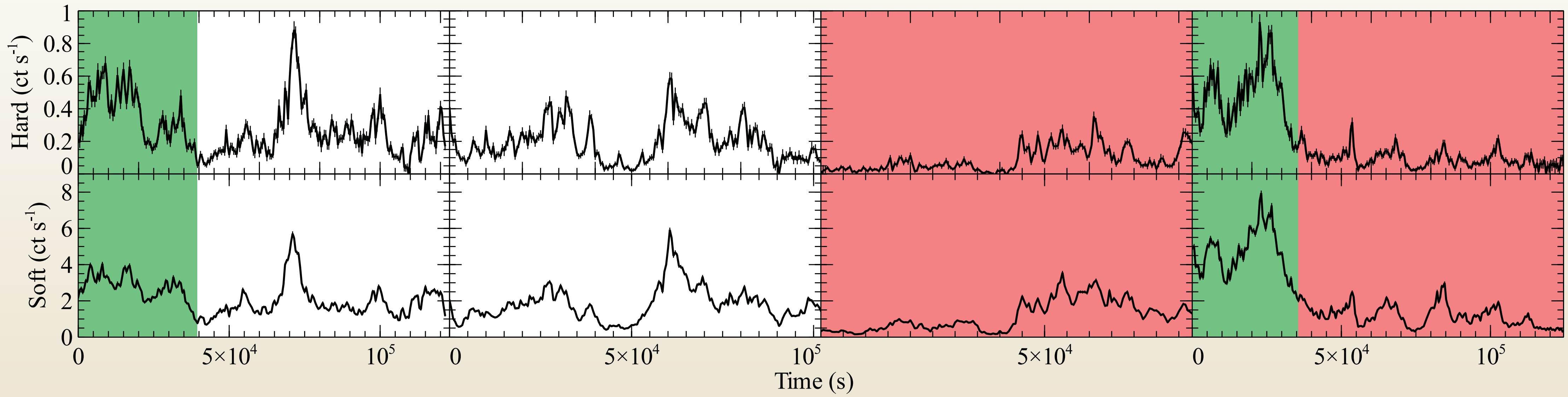

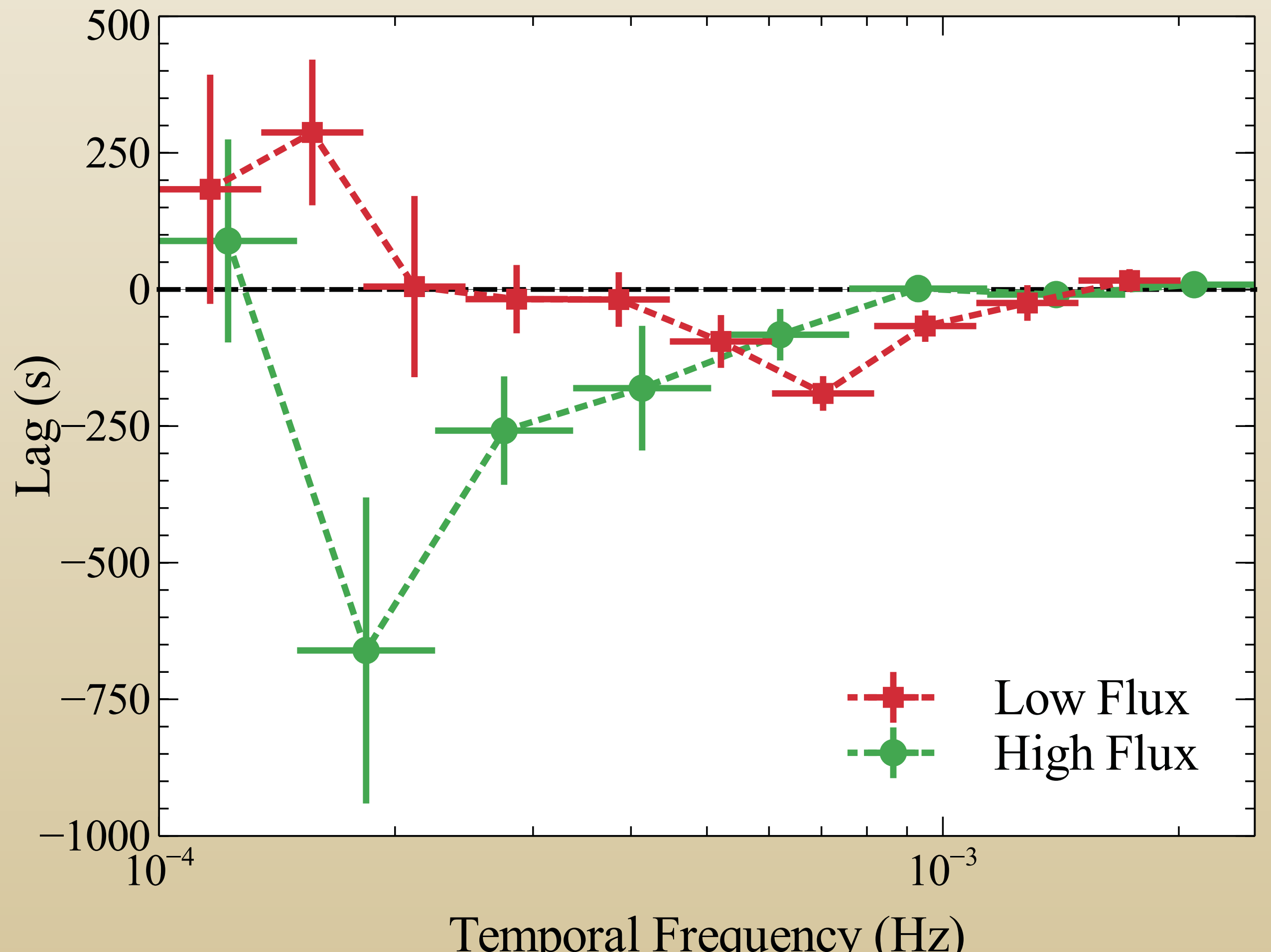

- hard (1.2-5.0 keV); soft (0.3-1.0 keV)
- soft lag of hard band occurs on longer time scales
- corona more vertically extended during high-flux states

Kara et al. (2013)

Period selection

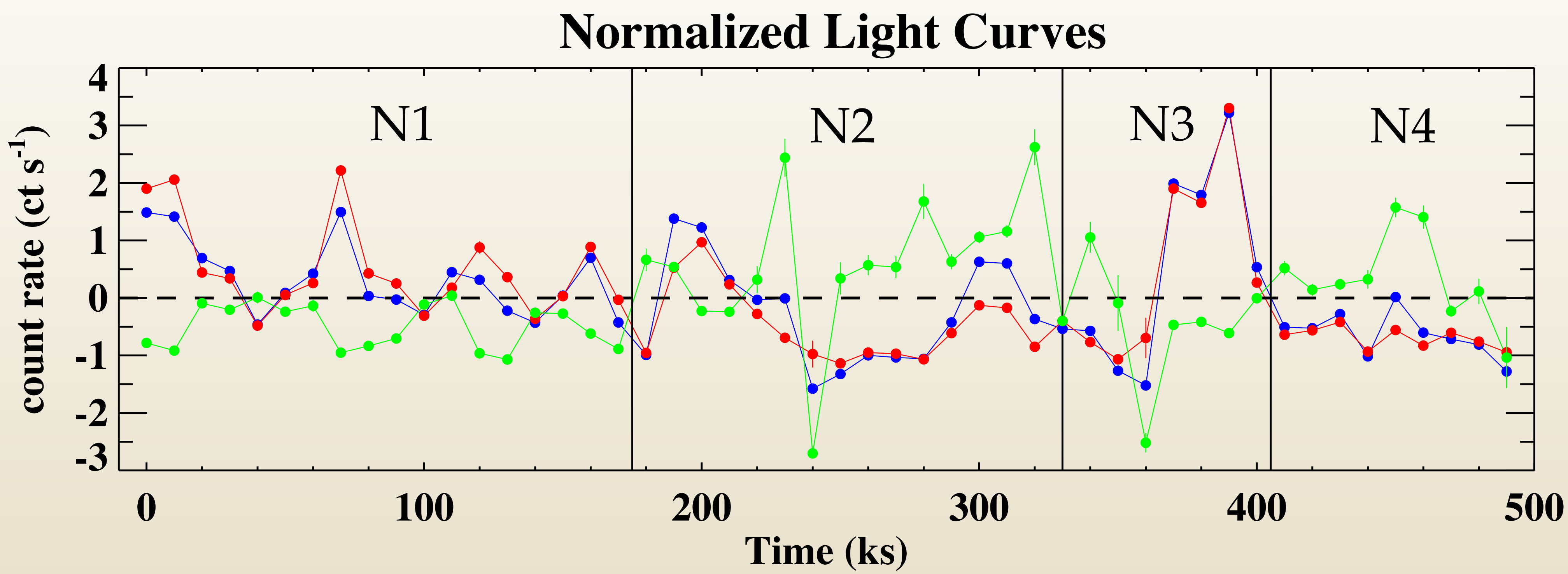

red (1.2-5.0 keV);
blue (0.3-1.0 keV);
green (blue/red)

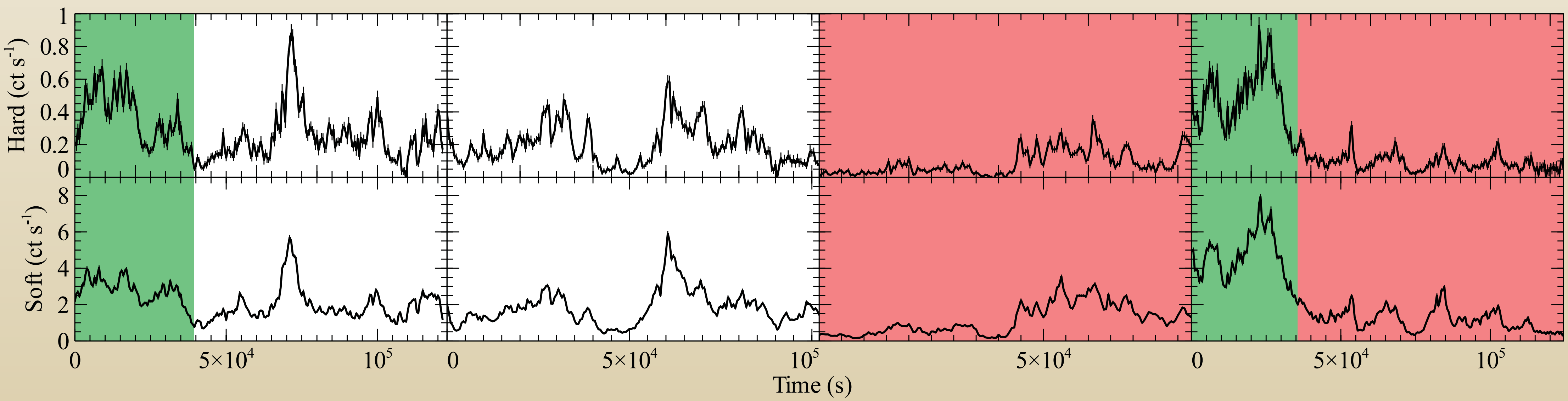

N1 & N3 ~ high-flux states (green)
N2 & N4 ~ low-flux states (red)
in Kara et al. (2013)

Time-resolved Spectra

Component	Parameter	Value			
		N1	N2	N3	N4
BBODY	kT (10^{-2} keV)	9.6 ± 0.2	$9.2^{+0.1}_{-0.2}$	9.6 ± 0.2	8.8 ± 0.2
	Norm	$3.9^{+0.3}_{-0.4} \times 10^{-5}$	$(4.0 \pm 0.1) \times 10^{-5}$	$4.9^{+0.6}_{-0.2} \times 10^{-5}$	$(3.0 \pm 0.1) \times 10^{-5}$
	F_{BB}	$32.4^{+2.2}_{-2.7}$	$33.4^{+0.9}_{-0.4}$	$41.3^{+3.2}_{-2.1}$	$25.2^{+0.8}_{-0.4}$
POWERLAW	Γ	2.69	2.63	2.80	2.63
	Norm	$(5.3 \pm 0.1) \times 10^{-4}$	$(2.2 \pm 0.1) \times 10^{-4}$	$7.4^{+0.2}_{-0.1} \times 10^{-4}$	$(1.4 \pm 0.1) \times 10^{-4}$
	F_{PLC}	$59.3^{+2.0}_{-3.4}$	23.4 ± 0.4	$93.7^{+1.6}_{-7.3}$	$14.5^{+0.3}_{-0.5}$
RELCONV	q	$3.8^{+0.4}_{-0.5}$	4.9 ± 0.2	$4.1^{+0.4}_{-0.6}$	$5.8^{+0.3}_{-0.4}$
EXTENDX	ξ_1	530 ± 70	500^{+10}_{-210}	830^{+190}_{-250}	500^{+100}_{-220}
	Norm_1	$1.4^{+0.3}_{-0.2} \times 10^{-8}$	$1.5^{+1.1}_{-0.2} \times 10^{-8}$	$1.5^{+0.7}_{-0.3} \times 10^{-8}$	$1.0^{+0.7}_{-0.1} \times 10^{-8}$
	$\mathcal{R}_1$	~ 0.27	~ 0.43	~ 0.30	~ 0.32
	Norm_2	$4.6^{+1.5}_{-1.1} \times 10^{-6}$	$3.7^{+0.2}_{-0.3} \times 10^{-6}$	$9.9^{+1.0}_{-3.0} \times 10^{-6}$	$5.6^{+0.2}_{-0.4} \times 10^{-6}$
	$\mathcal{R}_2$	~ 0.11	~ 0.13	~ 0.13	~ 0.33
	F_{RDC}	$36.5^{+5.8}_{-5.0}$	$29.8^{+0.6}_{-2.0}$	$69.9^{+6.2}_{-12.2}$	$27.2^{+2.8}_{-2.0}$
$\chi^2/d.o.f.$		1646/1475	1570/1225	1426/1194	1027/863

Time-resolved Spectra

Component	Parameter	Value			
		N1	N2	N3	N4
RELCONV	q	$3.8^{+0.4}_{-0.5}$	4.9 ± 0.2	$4.1^{+0.4}_{-0.6}$	$5.8^{+0.3}_{-0.4}$
EXTENDX	ξ_1	530 ± 70	500^{+10}_{-210}	830^{+190}_{-250}	500^{+100}_{-220}

$$\xi = L_{\rm ion}/nR^2$$

The corona is likely more **radially-extended** during high-flux states than low-flux states!

Summary

- Relativistic reflection model can explain the X-ray spectra of most AGN, including extreme sources.

- source geometry can be probed by combining results of timing and spectral analyses

- 1.5 Ms *XMM-Newton* data approved!

Thank you very much for your attention!